A Mechanism of Polarized Light Sensitivity in Cone Photoreceptors of the Goldfish *Carassius auratus*

Nicholas W. Roberts and Michael G. Needham
School of Physics and Astronomy, University of Manchester, Manchester, United Kingdom

ABSTRACT An integrated laser tweezer and microphotometry device has been used to characterize in detail how individual, axially orientated goldfish photoreceptors absorb linearly polarized light. This work demonstrates that the mid-wavelength sensitive members of double cone photoreceptors display axial differential polarization sensitivity. The polarization contrast was measured to be 9.2 ± 0.4%. By comparison, rod photoreceptors only exhibit isotropic absorbance. These data, combined with the square cone mosaic of double cones in the retina, suggest that intrinsic axial dichroism forms part of the underlying biophysical detection mechanism for polarization vision in this species.

INTRODUCTION

Polarized light vision is a common visual specialization found in both vertebrates and invertebrates (1–3). Polarized light exists in the visual environments of many animals as a result of scattering from the atmosphere or reflection and transmission at different surfaces such as water. To detect different polarization states of light, the individual light-sensitive cells in an animal's eye must be able to exhibit a differential polarization response (4,5). Several polarization detection mechanisms have been discovered among a variety of terrestrial and aquatic invertebrates (1,3,6–8). However, for vertebrates, the underlying biophysical mechanisms of polarization sensitivity remain unknown. While several studies have proposed different models (1,9–12), there has been no conclusive experimental evidence detailing the mechanism of polarization sensitivity in typical vertebrate photoreceptors.

There are two principal photoreceptor cell types in the vertebrate retina: rods and cones (13–15). The region of both cell types that contains the visual pigment is known as the outer segment, and in cones, it is formed from a continuous infolding of the cell plasma membrane. In rod outer segments, the corresponding membranes become pinched off into discrete double bilayer disks, separate from the plasma membrane and separate from each other. In general, it is believed that the underlying mechanism of polarization discrimination in vertebrate photoreceptors is not due to axial differential absorption in photoreceptor outer segments (1,15–17). This understanding stems from several experiments conducted by Brown (18) and Cone (19). They discovered that in multiple rods of a frog (*Rana pipiens*) the visual pigment undergoes rotational diffusion within the outer segment membranes. This implies that all axially incident polarized light will be absorbed isotropically. However, *R. pipiens* is not a species known to exhibit polarized light sensitivity. Moreover, it is known that only particular classes of cones, and not rods, provide the polarization-sensitive spectral channels in the visual system (1,20–23). To the authors' knowledge, there have been no published studies measuring rotational diffusion of the visual pigment or axial polarization absorbance in individual photoreceptors from a known polarization-sensitive species.

Primarily, axial absorbance data from single photoreceptors are lacking in the literature due to limitations in experimental measurement technology. For many years, the technique of microspectrophotometry (MSP) has proved the principal method for investigating how light, and polarized light in particular, is absorbed by individual photoreceptor cells (24–28). Common to all MSP measurements is the orientation geometry of the cells during the measurements. The sample preparation method results in all the photoreceptors lying in the plane of the sample, and as such, the absorbance is always measured transversely through the outer segment of the cell. However, only having the photoreceptors lying in the plane of the sample represents a significant drawback, since it prohibits any investigation into how individual rods and cones absorb axially incident polarized light, as they would do in the retina. This alignment issue has been the factor preventing any studies into the physiological axial absorbance of individual photoreceptors.

In this study, we report the first technique for measuring the axial absorbance of individual vertebrate rod or cone photoreceptors. By integrating a multi-trap laser tweezing and a microphotometry system, the orientation of individual cells has been controlled in three dimensions allowing axial absorbance measurements to be taken. This provides definitive information on the axial polarization absorbance from one photoreceptor, not an averaged measurement from multiple cell types. The results of this work show a significant difference between the way axially orientated rods and cones of goldfish, a species known to possess polarization vision (21), absorb linearly polarized light. The reported results illustrate that the mid-wavelength sensitive (MWS) part of the

Submitted May 9, 2007, and accepted for publication June 25, 2007.

Address reprint requests to N. W. Roberts, Tel.: 0161 2754236; E-mail: nicholas.roberts@manchester.ac.uk.

Editor: Janos K. Lanyi.

0006-3495/07/11/3241/08 $2.00

doi: 10.1529/biophysj.107.112292

double cone photoreceptor, one known to play a role in polarization vision (21), exhibits axial dichroism. Our findings demonstrate that combined with the arrangement of photoreceptors in the square cone mosaic, such axial dichroism could provide the basis of a polarization contrast detection system.

METHODS

Microphotometry laser tweezing system

The apparatus developed in this work introduces several new features additional to the typical MSP systems currently in use. The optical arrangement (shown schematically in Fig. 1) is centered on a Leitz DMIRB inverted microscope body (Leitz Microsystems, Montreal, Canada) and can be categorized into four main parts: 1), The measurement optics; 2), the detector system; 3), the optical tweezers; and 4), the viewing optics.

1. The measurement beam was produced at 532 nm by a 120-mW diode-pumped solid-state laser. Precise intensity control was achieved through an in-house liquid crystal device feedback system. The measurement beam was maintained at a stable photon rate of approximately one part in 10^3. A 4.5 neutral density filter reduced the intensity to $\sim 10^4$ photons s^{-1} at the back aperture of a 50× ULWD Olympus MPlan objective (Olympus, Melville, NY), which was used to focus the beam to a beam waist of <2 μm with a Rayleigh distance of ~ 10 μm.
2. The measurement beam was collected by a 100× Zeiss Neoplan oil immersion objective (NA 1.3; Carl Zeiss, Jena, Germany) and directed via a beamsplitter to a photomultiplier tube (Electron Tubes, Middlesex, UK). An amplifier and discriminator circuit connected the experiment to a PC running an in-house developed LabVIEW interface (National Instruments, Austin, TX).
3. The laser trapping system has been described previously (29). The optical trapping beam used in this setup was a 1 W Nd:YVO_4 1064-nm laser reduced in power via a neutral density filter setup to 110 mW measured at the back focal plane of the Zeiss objective. The principal advantages of using 1064 nm for photoreceptor work is this wavelength (and low power) causes no damage to the cell and does not bleach the visual pigment during the absorbance measurements (30). A standard relay lens system (*L1–L4* in Fig. 1) was employed to ensure the trapping beam entered the back aperture of the objective parallel to the principal axis of the lens. Two fast scanning goniometric-controlled mirrors (GSI Luminomics, Boston, MA) were used create the multiple traps with the positions controlled via the LabVIEW interface.
4. A background illumination was provided by a 980 nm laser (170 mW) coupled through an optical fiber to the microscope. Video images of the experiment were monitored in real time through the LabVIEW control software.

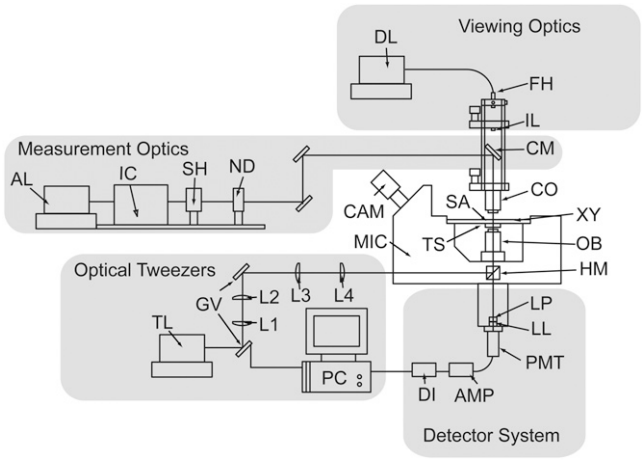

FIGURE 1 Schematic diagram of the laser tweezer microphotometer (*Measurement optics*: *AL*, absorbance 532-nm laser; *IC*, intensity controller; *SH*, shutter; and *ND*, neutral density filter. *Viewing optics*: *DL*, 980-nm diode illumination laser; *FH*, fiber holder; *IL*, collimating lens; *CM*, 45° cold mirror; *CO*, 50× ULWD Olympus MPlan objective; *SA*, sample; *TS*, temperature-controlled stage; *XY*, *x-y* stage; *MIC*, microscope body; *CAM*, video camera; *OB*, 100× Zeiss Neoplan oil immersion objective; and *HM*, 45° hot mirror. *Detector system*: *LP*, lowpass filter; *LL*, 532-nm laser line filter; *PMT*; photomultiplier tube; *AMP*, amplifier; and *DI*, discriminator. *Optical tweezers*: *TL*, 1064-nm trapping laser; *L1–L4*, beam steering lenses; and *GV*, galvanometer-controlled mirrors.)

Animals

Sample preparation methods were as described in Roberts et al. (12). Adult goldfish (*Carassius auratus*) were used with a mean body mass and size (±1 SD of the mean) of 7.1 ± 0.5 g and 6.8 ± 0.4 cm, respectively. Experimental measurements were carried out in a darkroom with no visible wavelength illumination. All fish were dark-adapted for 1 h before being euthanized by prolonged anesthesia with 100 mg l^{-1} Eugenol (Sigma, St. Louis, MO). Both eyes were excised, then hemisected and retina was removed in minimum essential medium (Sigma) under infrared light (980 nm). Sections of retina were teased apart onto a standard recessed microscope slide freeing individual photoreceptors. The recess was flooded with a small drop of minimum essential medium and a No. 1 coverslip was placed on top of the sample, and the edges sealed with clear nail varnish.

Statistical analysis

One-way ANOVA was used to determine differences between axial dichroic ratios. Null hypotheses were rejected at the 0.05 level. Values are expressed as mean ± SD.

MANIPULATING SINGLE PHOTORECEPTOR CELLS

Laser tweezers have been used in a wide range of studies to control and manipulate biological cells (31,32). With the correct choice of laser trapping wavelength and power, cells can be trapped without altering their properties or causing cellular damage. Recently, Townes-Anderson et al. (30) showed that vertebrate photoreceptors could be trapped, moved, and deposited in a controlled manner. Moreover, the cells were unaffected by being trapped, with photoreceptors deposited next to one another reconnecting intracellular processes.

Numerous laser trapping schemes have been devised to manipulate objects in two or three dimensions (33–37). A widely used method is to circularly polarize the trapping beam to transfer spin angular momentum to the sample, causing it to rotate (38,39). For out-of-plane manipulation, holographic tweezers or Bessel beam traps can be used to maneuver objects along the beam propagation direction. In fact, the anisotropic shape of cylindrical objects such as photoreceptor cells facilitates a simple method of controlling

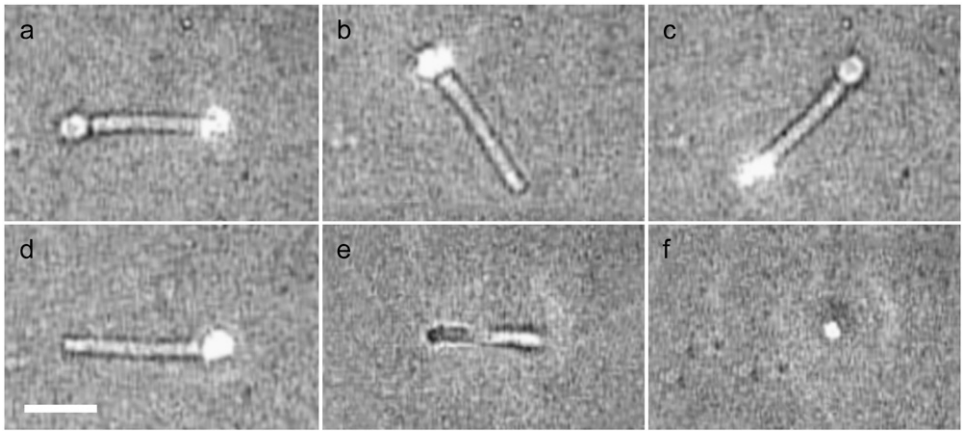

FIGURE 2 (*a–d*) A time series of video images illustrating a 180° rotation of a rod photoreceptor in the plane of the sample using a dual beam optical trap. (*e* and *f*) The controlled rotation of a rod photoreceptor using a single beam trap into its physiological end on orientation. Scale bar, 10 μm.

the three-dimensional orientation. Gauthier et al. (40) predicted theoretically and confirmed experimentally that cylinders transverse to the laser-beam axis undergo out-of-plane reorientation such that the long axis of the object becomes aligned with the propagation direction of the beam. However, if a single trap is located close to one of the ends of a cylinder, a transverse displacement of the beam will cause the object only to move in the plane of the sample because of the drag present on the nonilluminated end.

Following Gauthier's scheme, we have constructed a multi-trap laser system integrated into a microphotometry device as described in Methods. This has provided a method of simultaneously measuring absorbance while manipulating both rods and cones in three dimensions. Initially, a two-trap setup was used to displace each end of the cell in a required direction allowing the new technique to be validated in the context of previous transverse absorbance measurements. By rotating both traps in a circle, a single photoreceptor could be made to revolve around a defined center of rotation. Fig. 2, *a–d*, is an illustrative time series of images demonstrating this motion, with the two-trap system rotating a rod through 180° in the plane of the sample. By using just a single trap moved to the center of the cell and then refocused slightly, the long axis of the photoreceptor reorients parallel to the beam propagation direction (Fig. 2, *e* and *f*). Furthermore, by circularly polarizing the trapping beam, the single axially orientated cell could be made to rotate around the beam's axis.

All absorbance measurements were made using a linearly polarized laser at 532 nm. This wavelength was chosen to closely match the absorbance maximum values, λ_{max} for both rods and the MWS pigment in one outer segment of the double cones. Several studies (41–43) have measured the λ_{max} values of rods and MWS cones to be ~522 nm and 533 nm, respectively. The absorbance was measured by comparing a reference incident intensity, I_0, with a transmitted intensity, I, such that the absorbance, A, at each angle was then calculated as $A = \log I_0/I$ (44). I_0 was first measured through a clear part of the sample close to the photoreceptor of interest, as is the case with all single beam MSP devices.

MEASURING TRANSVERSE POLARIZATION ABSORBANCE

To place the results from this new measurement technique in the context of previous work, the transverse polarization absorbance of rod outer segments was initially examined. Fig. 3 illustrates a typical result, with the solid symbols representing the absorbance measured in the outer segment while the cell was rotated as described in Fig. 2, *a–e*, and with a step size of 5°. It should be noted that the full 360° rotation of the cell facilitates an important check. The measurements at 0, 180, and 360° represent repeated points where the absorbance geometry is the same. As can be seen from Fig. 3, these values (as they were in all other data sets reported here) are within 2 SD of each other, verifying that no detectable bleaching was occurring during the polarization

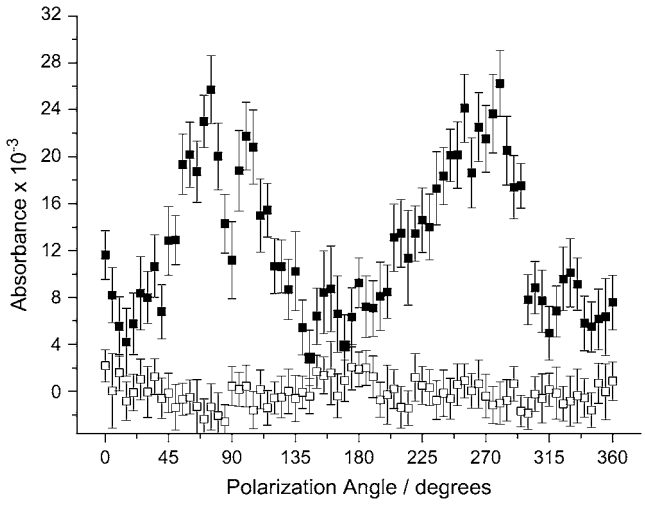

FIGURE 3 A typical example of an experimental linearly polarized transverse absorbance data set obtained from a rod (52) photoreceptor as it is rotated through 360° in the plane of the sample. The solid symbols clearly demonstrate the dichroic transverse absorbance of the outer segment. The open symbols illustrate the baseline post-bleach measurements. Error bars represent mean ±1 SD.

measurements. After the absorbance data for this sample had been taken, a further test was performed. Firstly, the neutral density filters were removed from the measurement beam and the same area of the outer segment was exposed to in excess of 10^8 photon s^{-1} for 5 min. Subsequently a post-bleach absorbance of the sample was then measured and is shown by the open symbols in Fig. 3. These data confirm that the measurements are recording the absorbance of the visual pigment and not an optical effect due to the rotation of the cell itself. Transverse absorbance measurements from 26 rod photoreceptors were used to calculate the mean transverse dichroic ratio (DR). Transverse dichroism arises in vertebrate outer segments by a combination of two mechanisms, intrinsic and form dichroism (45). Intrinsic dichroism occurs due to the in plane chromophore orientation within the transmembrane visual pigment. Form dichroism is caused by the lamellar structure of the outer segment membranes and the boundary conditions that such a structure imposes on the incident light. The transverse DR is defined as $DR = A_{\perp}/A_{\parallel}$, where $A_{\perp}$ and $A_{\parallel}$ are the absorbencies of light polarized linearly perpendicular and parallel to the long axis of the cell, respectively (44). The dichroic ratio at 532 nm was calculated to be 3.37 $\pm$ 0.42 (number of samples $n = 26$). It is worth noting that although DRs are typically quoted for the wavelength of maximum absorbance, theoretical (12,45) and experimental results (46) have shown the ratio to be wavelength-independent.

As described above, the measurement of the transverse DRs was conducted to validate our new experimental technique in the context of previous results. Initially, the transverse rod DR of 3.37 $\pm$ 0.42 appears somewhat higher then other values reported in the literature. Harosi and MacNichol (47) measured the DR of similar sized goldfish rods to be ~1–2, at 525–530 nm. However, vertebrate rod photoreceptors typically have DRs between 3 and 5 ((48) and references therein) with which our results do agree. In their study, Harosi and MacNichol (47) alluded to the fact that their DR values of 1–2 were reduced because of the increased scattering that occurs for smaller cells and a highly focused measurement beam. Our experimental system uses a linearly polarized 532 nm laser beam, and as such, is not subject to the same optics of other normal noncoherent white light microspectrophotometry devices such as that used by Harosi and MacNichol. The Gaussian laser beam of our system was set up to utilize a Rayleigh distance of ~10 μm at the beam waist. This effectively results in a collimated beam at the sample, and the absorbance measurements do not suffer from the same distortions that arise from a noncoherent strongly focused beam.

MEASURING AXIAL POLARIZATION ABSORBANCE

As described above, by circularly polarizing a single trapping beam, objects can be made to rotate through the transfer of spin angular momentum. In the second experiment reported here, we used such a system to make individual photoreceptor cells ''stand up end on'' into their physiological orientation and rotate. Fig. 4 *a* is a time series of video still images depicting the axial rotation of a double cone during an absorbance measurement, with the MWS outer segment at the center of rotation. The solid symbols in Fig. 4 *b* show the corresponding absorbance from this cell as the double cone rotated through the 180°. Clearly, the absorbance of linearly polarized light in MWS outer segments indicates a 180° periodic polarization sensitivity resulting in an axial linear dichroism. Again as an experimental check, a post-bleach absorbance data set was measured (*open symbols*), confirming that the dichroic measurements are indeed due to the visual pigment and not an artifact of the cell's rotation. Moreover, the Rayleigh distance of the measurement beam was still ~10 μm, a value greater than or equal to the length of the outer segment. This ensured again that the measurements were not subject to any of the distortions associated with high numerical aperture noncoherent optics. In contrast, Fig. 4, *c* and *d*, illustrates the rotation of a rod and a typical set of axial polarization absorbance measurements. Experimentally, it was more difficult to view the axial rotation of the rods due to their circular cross section. However, in the measurements made, there was enough nonuniformity in the image to view the rotation directly and correlate the rotation angle with position of the absorbance measurement. Moreover, the rotation was checked for being on-axis, by drawing a circular region of interest around the outer segment, and measuring for any departure to an elliptical cross section. These data in Fig. 4 *d* reveal that this rod exhibits a constant polarization absorbance around the axial rotation. Overall, in analyzing all the measurements performed (Fig. 4 *e*, $n = 9$ for both the rods and MWS cones), the mean axial DRs of the cells studied were calculated to be 1.04 $\pm$ 0.03 and 1.20 $\pm$ 0.09 for the rods and MWS cones, respectively. These results indicate that the axial DRs of rods and MWS cones are significantly different ($p < 0.05$; one-way ANOVA).

A MECHANISM OF POLARIZATION SENSITIVITY

Goldfish are a species known to possess polarization vision, mediated by their ultraviolet, mid- and long-wavelength sensitive pigments (21). Both Bernard and Wehner (4) and more recently Coughlin and Hawryshyn (5) discussed the requirements for polarization vision. The initial prerequisite is a first-stage detector mechanism to analyze the electric field vector of the incident light. Axial dichroism in a photoreceptor outer segment provides a direct way to achieve this, the differential output from the cell then matching the dichroic absorption. With the correct opponent processing of these cellular outputs from orthogonal channels, unique information can be obtained about the surrounding polarization field. Importantly, goldfish do possess an orthogonal photoreceptor mosaic (49). Furthermore, several studies of

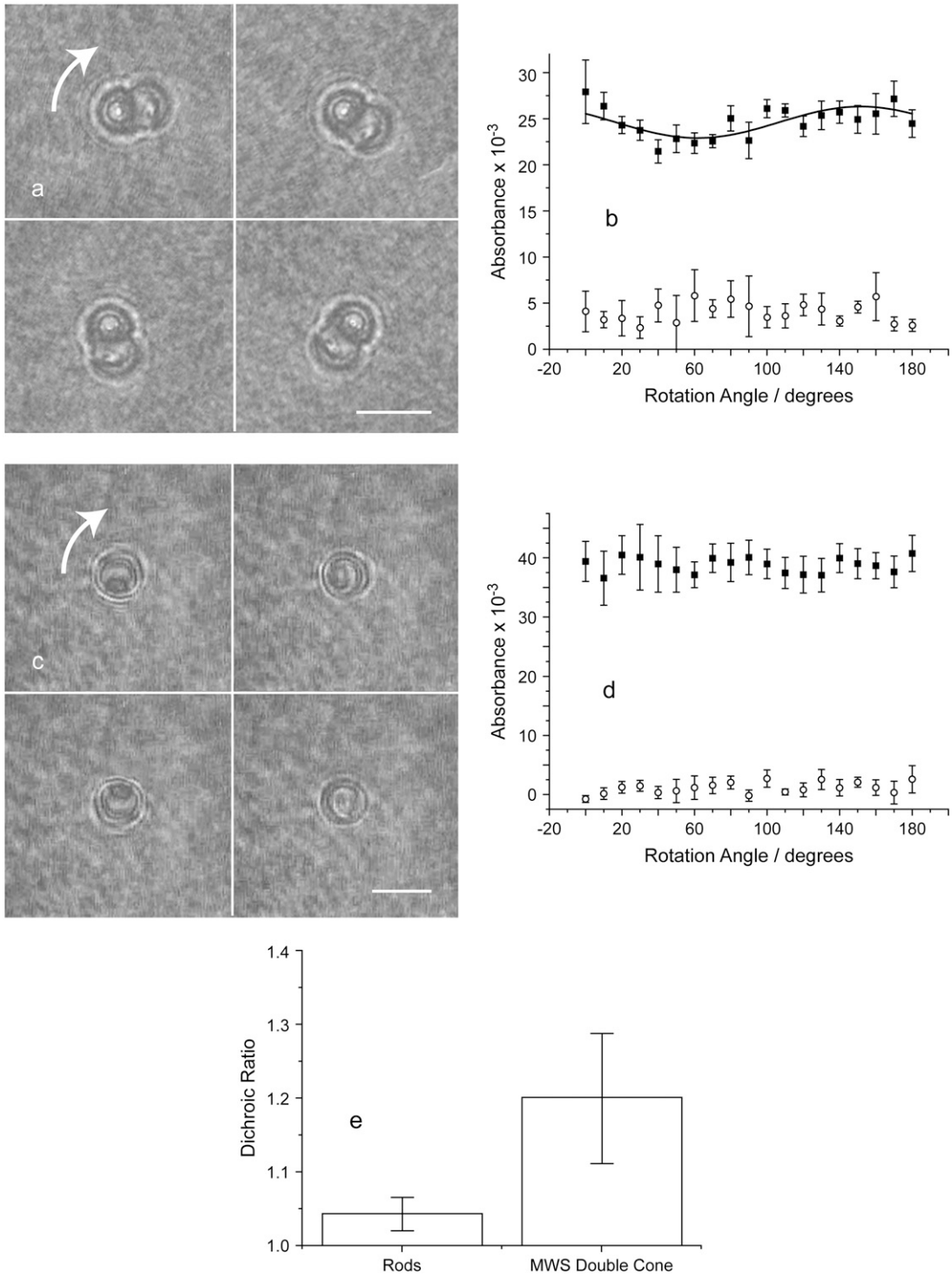

FIGURE 4 (*a*) A time series of video images illustrating a 180° rotation of an axially orientated double cone photoreceptor. The rotation is centered on the mid-wavelength sensitive (MWS) outer segment. Scale bar, 10 μm. (*b*) A typical set of axial absorbance measurements from an MWS outer segment indicating the axial dichroism of the cell type. (*c*) A time series of video images illustrating a 360° rotation of an axially orientated rod photoreceptor. Scale bar, 5 μm. (*d*) The corresponding constant axial absorbance measurements from a rotating rod photoreceptor. In panels *b* and *d*, the solid symbols represent the absorbance and the open symbols show the post-bleach baseline. (*e*) The mean axial dichroic ratios from all measured rods and MWS cones. The mean values are significantly different between cell types ($n = 9$; $p < 0.05$; one-way ANOVA). Error bars represent mean ± 1 SD.

other teleost species have established that such a square cone mosaic and the presence of the UV corner cones seems a common requirement for polarized light sensitivity (10,50). Therefore, an important implication of these experimental results is that the measured axial dichroism in the MWS part of the double cones fits all the criteria required to form part of the biophysical mechanism of polarized light sensitivity.

Clearly these measurements of axial dichroism seem in contradiction to the accepted understanding. Based on the rotational diffusion studies of the literature (18,19), the polarization absorbance should be invariant as a function of axial rotation in any photoreceptor type. Significantly though, and as described in the Introduction, the studies by Brown (18) and Cone (19) were conducted on *R. pipiens*, a species not known to possess any form of polarization sensitivity. Moreover, their data detailing the rotational diffusion was collected from small retina sections, not single axially orientated photoreceptors. As the retina of *R. pipiens* contains a majority of rods, isotropic axial absorption from such a bulk measurement only describes rotational diffusion in rods and therefore agrees with our results in single rods of the goldfish.

One of the hypotheses that has been proposed to explain polarization sensitivity in double cones relies on the inner segments acting as a polarization analyzer (9). Cameron and Pugh (9) suggested that the elliptical cross-section and gradient in refractive index of the inner segments would cause a differential transmission of orthogonal polarizations. This would result in different intensities reaching the outer segments, and coupled to the orthogonal arrangement of a double cone mosaic, unambiguous polarization information could be obtained. However, all the post-bleach measurements recorded in this work (see Fig. 4 *e*) suggest that experimentally, this is not the case. Any differences in polarization transmission through the inner segments would modulate the measured intensity and thus the flat baselines seen in these data show there is no differential transmission through the inner segments.

Two possible mechanisms which could underlie axial dichroism rely on the outer segment structure or membrane order to provide a detector mechanism (12,48). The typical structure of the outer segment has the plane of the membranes transverse within the cell. However, any tilt to those membranes would result in an axial dichroism. Indeed, a unique limiting case where the tilt equals 90° is known to exist in the atypical bilobed cones of *Anchoa sp.*, which exhibit a dichroic ratio of ~1.5 (16). In support of a tilted membrane hypothesis, we have previously presented work (12) indicating that all spectral classes' cones of *Oncorhynchus kisutch*, a teleost that exhibits a similar polarization sensitivity, have a tilted optical structure. The analysis of those results indicated that the polarization contrast, defined as $A_{max} - A_{min}/A_{max} + A_{min}$, where A_{max} and A_{min} are the orthogonal maximum and minimum axial absorbencies, was ~10%. In this study, the measured polarization contrast of the MWS outer segments in goldfish is similar, equal to 9.2 ± 0.4%.

A second possibility that cannot be discounted, concerns the lipid composition of the outer segment membranes and differences that occur between cell types. Recent investigations have shown that rod disks and the surrounding outer cell membrane differ significantly in lipid makeup. For example, the plasma membrane has considerably higher levels of cholesterol and the ratio of saturated to unsaturated fatty acids is markedly different (51). Suggestions have been made that the lipid composition in cones mirrors that of the rod outer cell membrane due to the infolding outer cell membrane (52). Such compositional differences not only affect rates of phototransduction (53) but properties such as the rotational viscosity and phase order (54). Any increase in viscosity of the bilayers leads to a corresponding reduction in rotational diffusion, which in turn could induce intrinsic dichroism subject to a level of biaxiality within the membranes. Indeed, Corless et al. (55,56) have already described several cases of higher degrees of in-plane order in certain cone outer segments. Certainly, the compositional differences that underlie the specifics of selective function in different cell types is an important area that could yet yield further results for understanding polarization vision.

CONCLUSIONS

To summarize, we have reported the first controlled axial absorbance measurements in single vertebrate photoreceptor cells. A multi-trap laser tweezer system has been used to manipulate individual cells in three dimensions while the polarization absorbance was measured. We have shown that the MWS part of double cones in goldfish is axially linearly dichroic. In the context of polarization vision, the axial dichroism and levels of polarization contrast measured, combined with the ordered photoreceptor mosaic, will provide direct polarization information to the next stage of neural processing. As such, this first stage of discrimination forms part of the biophysical mechanism underlying polarized light detection in this species. For the future, the integration of manipulation and measurement technologies such as demonstrated by this work opens up the possibility of new research. In particular, such a setup combining three-dimensional cell manipulation and spectral absorbance measurements could be easily advanced to allow the investigation of the true physiological optical properties of different vertebrate photoreceptor types.

The authors thank H.F. Gleeson and M.R. Dickinson for providing the laser tweezing equipment.

This work was supported by the Leverhulme Trust and the Engineering and Physical Sciences Research Council.

REFERENCES

1. Horváth, G., and D. Varjú. 2004. Polarized Light in Animal Vision. Springer, Berlin, Heidelberg.

2. Wehner, R. 2001. Polarization vision—a uniform sensory capacity? *J. Exp. Biol.* 204:2589–2596.
3. Waterman, T. H. 1981. Polarization sensitivity. *In* Handbook of Sensory Physiology, Vol. VII/6B. Springer-Verlag, Berlin, Heidelberg, New York.
4. Bernard, G. D., and R. Wehner. 1977. Functional similarities between polarization vision and color vision. *Vision Res.* 17:1019–1028.
5. Coughlin, D. J., and C. W. Hawryshyn. 1995. A cellular basis for polarized-light vision in rainbow trout. *J. Comp. Physiol.* [*A*]. 176:261–272.
6. Wehner, R. 1976. Polarized-light navigation by insects. *Sci. Am.* 235: 106–115.
7. Marshall, N. J., M. F. Land, C. A. King, and T. W. Cronin. 1991. The compound eyes of mantis shrimps (*Crustacea*, *Hoplocarida*, *Stomatopoda*). 1. Compound eye structure—the detection of polarized light. *Philos. Trans. R. Soc. Lond. B Biol. Sci.* 334:33–56.
8. Shashar, N., and T. W. Cronin. 1996. Polarization contrast vision in Octopus. *J. Exp. Biol.* 199:999–1004.
9. Cameron, D. A., and E. N. Pugh. 1991. Double cones as a basis for a new type of polarization vision in vertebrates. *Nature*. 353:161–164.
10. Flamarique, I. N., C. W. Hawryshyn, and F. I. Harosi. 1998. Double-cone internal reflection as a basis for polarization detection in fish. *J. Opt. Soc. Am. A Opt. Image Sci. Vis.* 15:349–358.
11. Hawryshyn, C. W. 2000. Ultraviolet polarization vision in fishes: possible mechanisms for coding E-vector. *Philos. Trans. R. Soc. Lond. B Biol. Sci.* 355:1187–1190.
12. Roberts, N. W., H. E. Gleeson, S. E. Temple, T. J. Haimberger, and C. W. Hawryshyn. 2004. Differences in the optical properties of vertebrate photoreceptor classes leading to axial polarization sensitivity. *J. Opt. Soc. Am. A Opt. Image Sci. Vis.* 21:335–345.
13. Cohen, A. I. 1972. Rods and cones. *In* Handbook of Sensory Physiology, Vol. VII/2. Springer, Berlin, Heidelberg, New York.
14. Fein, E., and A. Szuts. 1982. Photoreceptors: Their Role in Vision. Cambridge University Press, Cambridge, UK.
15. Land, M. F., and D.-E. Nilsson. 2001. Animal eyes. *In* Oxford Animal Biology Series. Oxford University Press, New York.
16. Flamarique, I. N., and F. I. Harosi. 2002. Visual pigments and dichroism of anchovy cones: a model system for polarization detection. *Vis. Neurosci.* 19:467–473.
17. Land, M. F. 1991. Vision—polarizing the world of fish. *Nature*. 353: 118–119.
18. Brown, P. K. 1972. Rhodopsin rotates in visual receptor membrane. *Nature New Biol.* 236:35–38.
19. Cone, R. A. 1972. Rotational diffusion of rhodopsin in visual receptor membrane. *Nature New Biol.* 236:39–42.
20. Flamarique, I. N., and C. W. Hawryshyn. 1998. Photoreceptor types and their relation to the spectral and polarization sensitivities of Clupeid fishes. *J. Compar. Physiol. A Sensory Neural Behav. Physiol.* 182:793–803.
21. Hawryshyn, C. W., and W. N. McFarland. 1987. Cone photoreceptor mechanisms and the detection of polarized light in fish. *J. Compar. Physiol. A Sensory Neural Behav. Physiol.* 160:459–465.
22. Parkyn, D. C., and C. W. Hawryshyn. 1993. Polarized-light sensitivity in rainbow trout (*Oncorhynchus-Mykiss*)—characterization from multiunit responses in the optic nerve. *J. Compar. Physiol. A Sensory Neural Behav. Physiol.* 172:493–500.
23. Parkyn, D. C., and C. W. Hawryshyn. 2000. Spectral and ultraviolet-polarization sensitivity in juvenile salmonids: a comparative analysis using electrophysiology. *J. Exp. Biol.* 203:1173–1191.
24. Harosi, F. I., and E. F. MacNichol. 1974. Dichroic microspectrophotometer—computer-assisted, rapid, wavelength-scanning photometer for measuring linear dichroism in single cells. *J. Opt. Soc. Am.* 64: 903–918.
25. Bowmaker, J. K. 1984. Microspectrophotometry of vertebrate photoreceptors—a brief review. *Vision Res.* 24:1641–1650.
26. Bowmaker, J. K., A. Thorpe, and R. H. Douglas. 1991. Ultraviolet-sensitive cones in the goldfish. *Vision Res.* 31:349–352.
27. Robinson, J., E. A. Schmitt, F. I. Harosi, R. J. Reece, and J. E. Dowling. 1993. Zebrafish ultraviolet visual pigment—absorption-spectrum, sequence, and localization. *Proc. Natl. Acad. Sci. USA.* 90:6009–6012.
28. Govardovskii, V. I., N. Fyhrquist, T. Reuter, D. G. Kuzmin, and K. Donner. 2000. In search of the visual pigment template. *Vis. Neurosci.* 17:509–528.
29. Gleeson, H. F., T. A. Wood, and M. Dickinson. 2006. Laser manipulation in liquid crystals: an approach to microfluidics and micromachines. *Philos. Trans. Roy. Soc. A Math. Phys. Eng. Sci.* 364: 2789–2805.
30. Townes-Anderson, E., R. S. St. Jules, D. M. Sherry, J. Lichtenberger, and M. Hassanain. 1998. Micromanipulation of retinal neurons by optical tweezers. *Mol. Vis.* 4:12.
31. Molloy, J. E., and M. J. Padgett. 2002. Lights, action: optical tweezers. *Contemp. Phys.* 43:241–258.
32. Molloy, J. E., K. Dholakia, and M. J. Padgett. 2003. Preface: optical tweezers in a new light. *J. Mod. Opt.* 50:1501–1507.
33. Paterson, L., M. P. MacDonald, J. Arlt, W. Sibbett, P. E. Bryant, and K. Dholakia. 2001. Controlled rotation of optically trapped microscopic particles. *Science*. 292:912–914.
34. Arlt, J., V. Garces-Chavez, W. Sibbett, and K. Dholakia. 2001. Optical micromanipulation using a Bessel light beam. *Optics Comm.* 197: 239–245.
35. O'Neil, A. T., and M. J. Padgett. 2002. Rotational control within optical tweezers by use of a rotating aperture. *Opt. Lett.* 27:743–745.
36. Bingelyte, V., J. Leach, J. Courtial, and M. J. Padgett. 2003. Optically controlled three-dimensional rotation of microscopic objects. *Appl. Phys. Lett.* 82:829–831.
37. Mohanty, S. K., R. Dasgupta, and P. K. Gupta. 2005. Three-dimensional orientation of microscopic objects using combined elliptical and point optical tweezers. *Appl. Phys. B*. 81:1063–1066.
38. He, H., M. E. J. Friese, N. R. Heckenberg, and H. Rubinsztein-Dunlop. 1995. Direct observation of transfer of angular-momentum to absorptive particles from a laser-beam with a phase singularity. *Phys. Rev. Lett.* 75:826–829.
39. Simpson, N. B., K. Dholakia, L. Allen, and M. J. Padgett. 1997. Mechanical equivalence of spin and orbital angular momentum of light: an optical spanner. *Opt. Lett.* 22:52–54.
40. Gauthier, R. C., M. Ashman, and C. P. Grover. 1999. Experimental confirmation of the optical-trapping properties of cylindrical objects. *Appl. Opt.* 38:4861–4869.
41. Harosi, F. I. 1976. Spectral relations of cone pigments in goldfish. *J. Gen. Physiol.* 68:65–80.
42. Stell, W. K., and F. I. Harosi. 1976. Cone structure and visual pigment content in retina of goldfish. *Vision Res.* 16:647–657.
43. Parry, J. W. L., and J. K. Bowmaker. 2000. Visual pigment reconstitution in intact goldfish retina using synthetic retinaldehyde isomers. *Vision Res.* 40:2241–2247.
44. Harosi, F. I. 1982. Polarized microspectrophotometry for pigment orientation and concentration. *Methods Enzymol.* 81:642–647.
45. Roberts, N. W. 2006. The optics of vertebrate photoreceptors: anisotropy and form birefringence. *Vision Res.* 46:3259–3266. http://dx.doi.org/10.1016/j.visres.2006.03.019.
46. Harosi, F. I. 1987. *Cynomolgus* and Rhesus-monkey visual pigments—application of Fourier-transform smoothing and statistical techniques to the determination of spectral parameters. *J. Gen. Physiol.* 89:717–743.
47. Harosi, F. I., and E. F. MacNichol. 1974. Visual pigments of goldfish cones—spectral properties and dichroism. *J. Gen. Physiol.* 63:279–304.
48. Roberts, N. W., and H. F. Gleeson. 2004. The absorption of polarized light by vertebrate photoreceptors. *Vision Res.* 44:2643–2652. http://dx.doi.org/10.1016/j.visres.2004.06.001.

49. Marc, R. E., and H. G. Sperling. 1976. Chromatic organization of goldfish cone mosaic. *Vision Res.* 16:1211–1224.

50. Flamarique, I. N., and C. W. Hawryshyn. 1998. The common white sucker (*Catostomus commersoni*): a fish with ultraviolet sensitivity that lacks polarization sensitivity. *J. Compar. Physiol. A Neuroethol. Sensory Neural Behav. Physiol.* 182:331–341.

51. Boesze-Battaglia, K., and R. J. Schimmel. 1997. Cell membrane lipid composition and distribution: implications for cell function and lessons learned from photoreceptors and platelets. *J. Exp. Biol.* 200:2927–2936.

52. Albert, A. D., and K. Boesze-Battaglia. 2005. The role of cholesterol in rod outer segment membranes. *Prog. Lipid Res.* 44:99–124.

53. Albert, A. D., J. E. Young, and P. L. Yeagle. 1996. Rhodopsin-cholesterol interactions in bovine rod outer segment disk membranes. *Biochim. Biophys. Acta Biomembr.* 1285:47–55.

54. Yeagle, P. L. 1985. Cholesterol and the cell-membrane. *Biochim. Biophys. Acta.* 822:267–287.

55. Corless, J. M., E. Worniallo, and R. D. Fetter. 1994. Three-dimensional membrane crystals in amphibian cone outer segments. 1. Light-dependent crystal-formation in frog retinas. *J. Struct. Biol.* 113:64–86.

56. Corless, J. M., E. Worniallo, and T. G. Schneider. 1995. Three-dimensional membrane crystals in amphibian cone outer segments. 2. Crystal type associated with the saddle-point regions of cone disks. *Exp. Eye Res.* 61:335–349.